Crossover from commensurate to incommensurate antiferromagnetism in stoichiometric NaFeAs revealed by single-crystal ^{23}Na,^{75}As-NMR experiments

Kentaro KITAGAWA[1,2*], Yuji MEZAKI[1,3], Kazuyuki MATSUBAYASHI[1,2], Yoshiya UWATOKO[1,2], and Masashi TAKIGAWA[1,2]

[1]*Institute for Solid State Physics, University of Tokyo, 5-1-5 Kashiwanoha, Kashiwa, Chiba 277-8581, Japan*
[2]*JST, TRIP, 5 Sanbancho, Chiyoda, Tokyo 102-0075, Japan*
[3]*College of Science and Technology, Nihon University, Kanda-Surugadai 1-8, Chiyoda-ku, Tokyo 101-8308, Japan*

We report results of ^{23}Na and ^{75}As nuclear magnetic resonance (NMR) experiments on a self-flux grown high-quality single crystal of stoichiometric NaFeAs. The NMR spectra revealed a tetragonal to twinned-orthorhombic structural phase transition at $T_{\rm O} = 57$ K and an antiferromagnetic (AF) transition at $T_{\rm AF} = 45$ K. The divergent behavior of nuclear relaxation rate near $T_{\rm AF}$ shows significant anisotropy, indicating that the critical slowing down of stripe-type AF fluctuations are strongly anisotropic in spin space. The NMR spectra at low enough temperatures consist of sharp peaks showing a commensurate stripe AF order with a small moment $\sim$0.3 μB. However, the spectra just below $T_{\rm AF}$ exhibits highly asymmetric broadening pointing to an incommensurate modulation. The commensurate-incommensurate crossover in NaFeAs shows a certain similarity to the behavior of $SrFe_2As_2$ under high pressure.

KEYWORDS: NaFeAs, NMR, incommensurate antiferromagnetism, 111-type iron arsenide

Stripe-type antiferromagnetic (AF) order has been commonly observed on the undoped or low-pressure region in the phase diagrams of iron-based superconductivities. Thus AF fluctuations are often considered the driving force for superconducting (SC) paring.[1)] For example, the $s_{\pm}$-wave pairing state, where the order parameter changes sign between the nested electron and hole Fermi surfaces, can be stabilized by the interband AF fluctuations.[2)] Since the geometry of the Fermi surfaces depends on materials and changes with doping, the nesting wave vectors may deviate from the commensurate (C) conditions in some cases, leading to incommensurate (IC)-AF order, or in other words, spin-density-wave (SDW) order in a narrow sense.

However, all the AF orders of the undoped stoichiometric compounds so far are known to be C-type.[3)] IC order has been reported for some non-stoichiometric or chemically doped materials. Neutron scattering experiments on the lightly electron-doped systems $Fe_{1+\delta}Te_{1-x}Se_x$ reported short-ranged IC order characterized by broad magnetic peaks off-centered from the commensurate wave vectors.[4,5)] IC-SDW order has been also reported for $Ba(Fe_{1-x}Co_x)_2As_2$ by NMR[6)] and Mössbauer[7)] experiments. However, microscopic disorder in these materials should bring distribution in the magnitude of ordered moments, which might be difficult to distinguish from incommensuration due to Fermi surface nesting. Therefore, finding a stoichiometric material exhibiting IC-SDW would mark important advance in our understanding of magnetism in iron-pnictide materials.

Among different types of iron-based superconductors, 122-type AFe_2As_2 (A=Ca, Sr, Ba) have been attracting strong interest because large single crystals with stoichiometric composition can be grown. Recently 111-type materials, LiFeAs and NaFeAs (Fig. 1a), have also been found suitable for crystal growth with alkaline-rich self flux.[8,9)] LiFeAs is a bulk superconductor with the transition temperature $T_{\rm SC}$ of 17 K,[10)] while NaFeAs shows only filamentary superconductivity.[11,12)] NaFeAs shows successive phase transitions: tetragonal-to-orthorhombic structural transition at $T_{\rm O} \sim 50$ K and AF transition at $T_{\rm AF} \sim 40$ K.[8,12)] The transition temperatures, which are significantly lower than those for 1111 and 122 materials,[3)] seem to depend sensitively on self-doping due to Na deficiency or synthetic methods.[12)] In this letter, we report observation of IC-AF order and a temperature-driven IC-C crossover in stoichiometric NaFeAs by NMR experiments on ^{23}Na and ^{75}As nuclei.

The crystals of NaFeAs were grown by the self-flux method with starting elemental ratio of 2:1:2. The materials were put into alumina crucible, sealed in a doubled-wall quartz tube in argon atmosphere, and heated to 900°C. Crystals grew during subsequent cooling down to 400°C in three days, then to room temperature in one day. We confirmed 1:1:1 atomic content within 2% by energy dispersive X-ray spectroscopy. Resistivity, magnetization and specific heat measurements detected the successive transitions at $T_{\rm O} = 57$ K and $T_{\rm AF} = 45$ K. The values of $T_{\rm O}$ and $T_{\rm AF}$ of our crystal, also confirmed by the NMR experiments as described below, are significantly higher than the previous reports,[11,12)] indicating less self-doping. The c-axis length measured by single-crystal x-ray diffraction was 7.05 Å at room temperature, which is longer than the previous reports. The crystal ($5 \times 3 \times 0.3$ mm^3) was handled in purified argon and covered with grease before exposed to air for mounting on the NMR probe equipped with a double-axis goniometer. The NMR spectra were acquired using Fourier step summing technique. The Fourier transformed spectrum of spin-echo was accumulated at shifted frequencies while the frequency or magnetic field was

*kitag@issp.u-tokyo.ac.jp

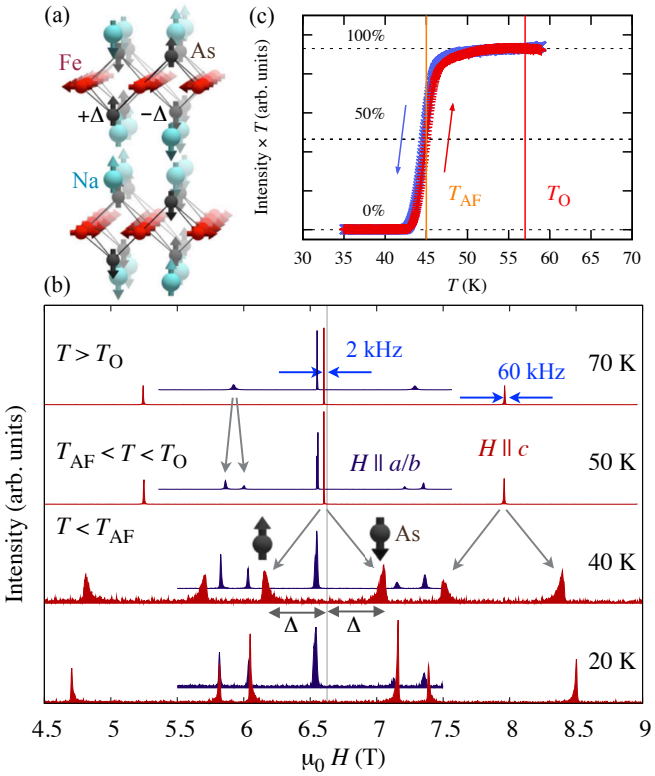

Fig. 1. (Color online) (a) Crystal structure and stripe-type antiferromagnetic order (red arrows) of NaFeAs. The arrows at As and Na nuclei indicate the hyperfine field in the antiferromagnetic state. (b) Field-swept ^{75}As-NMR spectra at 48.31 MHz. Below T_O, the satellite lines for $H \perp c$ splits into two sets due to twining. Below T_{AF}, the center line for $H \parallel c$ splits symmetrically by the hyperfine fields parallel to the c axis at the As sites. The dotted line shows the unshifted resonance field. The full widths at the half maxima (enclosed by the arrows) are narrower than those for 122 parent compounds,[13,14] indicating good stoichiometry of the sample. (c) Temperature dependence of the intensity at the peak position of the paramagnetic spectrum multiplied by T for $H \parallel c$. No hysteresis was observed across T_{AF}, except for the small instrumetal delays.

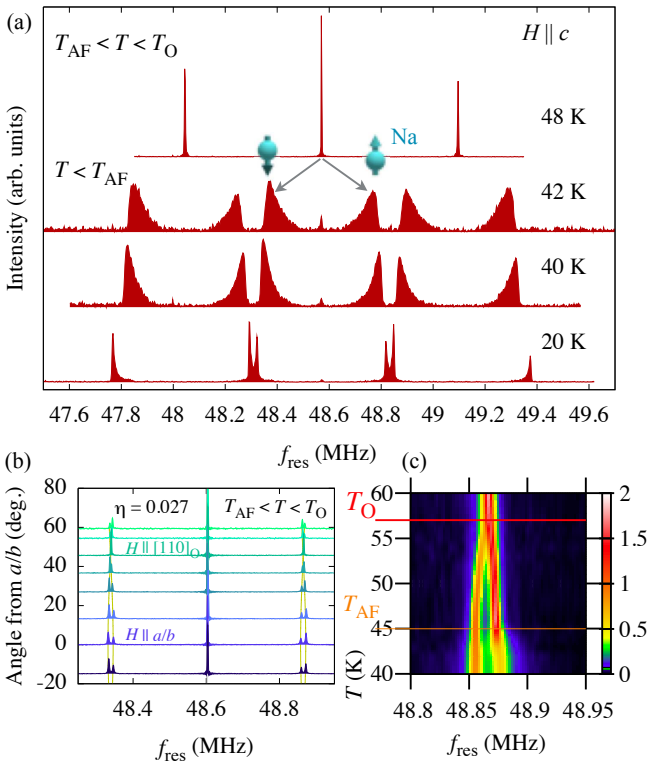

Fig. 2. (Color online) Frequency-swept ^{23}Na-NMR spectra at 4.25 T (a) for $H \parallel c$ at different temperatures and (b) for $H \perp c$ along various directions in the ab-plane at $T = 50$ K. The spectra for $H \parallel c$ show incommensurate modulation immediately below T_{AF}. The satellite lines are doubled for $H \perp c$ due to twinning in the orthorhombic structure. Their angular dependence in the ab-plane is well reproduced by eq. (2) with $\eta = 0.027$ (dashed lines). (c) A color plot of the satellite intensity as a function of temperature for $H \parallel a$ or b, showing the tetragonal-to-orthorhombic structural transition at $T_O = 57$ K.

being swept. NMR relaxation rates T_1^{-1} were determined by the inversion recovery method. Good fitting to the theoretical recovery curve for spin $I = 3/2$ nuclei, $\{\exp(-t/T_1) + 9\exp(-6t/T_1)\}/10$, was obtained in the whole temperature range.

The NMR spectra are shown in Fig. 1(b) for ^{75}As nuclei and in Fig. 2 for ^{23}Na nuclei. Both As and Na occupy the same type of site, the $2c$ site in the high-T tetragonal $P4/nmm$ structure and the $4g$ site in the low-T orthorhombic $Cmma$ structure. Since both nulcei have spin 3/2, the NMR spectra consist of quadrupole-split three lines with the resonance frequencies (here up to the first-order perturbation of the quadrupole interaction).

$$f_{\rm res} = \mu_0 \gamma_{\rm N} H_{\rm eff} + i\delta\nu \quad (i = -1, 0, 1), \tag{1}$$

where $\gamma_{\rm N}$ is the nuclear gyromagnetic ratio ($2\pi \times 7.29019$ MHz/T for ^{75}As and $2\pi \times 11.26226$ MHz/T for ^{23}Na), $\boldsymbol{H}_{\rm eff} = \boldsymbol{H}_{\rm ext} + \boldsymbol{H}_{\rm hf}$ is the sum of the external field and the magnetic hyperfine field, and

$$\delta\nu = \frac{\nu^c}{2}\left(3\cos^2\theta - 1 + \eta\sin^2\theta\cos 2\phi\right), \tag{2}$$

is the quadrupole splitting. Here, (θ, ϕ) specifies the polar angle of $\boldsymbol{H}_{\rm eff}$ with respect to the c-axes and $\eta = |\nu^{aa} - \nu^{bb}|/|\nu^{cc}|$ is the asymmetry parameter of the electric field gradient (EFG) tensor $\nu_{\alpha\alpha}$. In the tetragonal $P4/nmm$ structure, η must be zero. While the center line ($i = 0$) is determined only by the magnetic hyperfine field, therefore, provides direct information on the spin structure, the satellite lines ($i = \pm 1$) are affected by EFG which is a sensitive probe for structural transitions.

The ^{75}As-NMR spectrum at 70 K (Fig. 1b) shows three lines for both $H \parallel c$ and $H \perp c$ as expected. At 50 K below T_O the satellite lines are doubled for $H \parallel a$ or $H \parallel b$ in the orthorhombic notation. This has been observed also in 122-type compounds and ascribed to nonzero η and twinned domains in the orthorhombic structure.[13,14] Details of the transition were investigated by ^{23}Na NMR (Fig. 2) providing better S/N ratio. The angular dependence of the satellite resonance frequencies in the ab-plane at 50 K (Fig. 2b) is well reproduced by Eq. (2) with $\eta = 0.027$ (dashed lines). The onset temperature for the splitting of the satellite lines (Fig. 2c) agrees with $T_O = 57$ K determined by the resistivity measurement.

The AF transition is marked by vanishing of the NMR line for $H \parallel c$ near the paramagnetic resonance field

below $T_{\rm AF} = 45$ K (Fig. 1c for ^{75}As). Absence of hysteresis indicates the transition is continuous. At sufficiently low temperatures, each of three lines split symmetrically into two lines for $H \parallel c$, but no line splitting occurs for $H \perp c$ [see the spectra at $T = 20$ K for ^{75}As (Fig. 1b) and ^{23}Na (Fig. 2a)]. This indicates staggered hyperfine fields at the As/Na sites along the c-direction $\boldsymbol{H}_{\rm hf} = (0, 0, \pm\Delta)$ with very small distribution of Δ. Following the analysis on the similar results for 122 compounds,[13,14] we conclude that the hyperfine field is generated by a stripe AF order with the q-vector $(1, 0, \frac{1}{2})_{\rm O}$ (defined on the orthorhombic $Cmna$ unit cell) and the AF moment along the a-axis (Fig. 1a). The off-diagonal element (B_{ac}) of the hyperfine coupling tensor relates the AF moment σ and Δ as $\Delta = 4B_{ac}\sigma$.[13] Assuming the same value $B_{ac} = 0.4 \sim 0.5$ T/$\mu_{\rm B}$ obtained for 122 compounds,[13,14] the AF moment in NaFeAs is estimated to be $0.28 \sim 0.34$ $\mu_{\rm B}$ at 20 K. This is close to the value reported by Yu *et al.* also from NMR experiments[11] but significantly larger than the value 0.09 ± 0.04 $\mu_{\rm B}$ obtained by neutron experiments.[12]

However, the spectral shape exhibits unusual temperature dependence near $T_{\rm AF}$. The narrow six lines of the ^{75}As NMR spectrum at 20 K develop asymmetric distribution at 40 K with a sharp edge at the maximum value of Δ (Fig. 1b). The sharp upper cutoff is unlikely to be caused by extrinsic disorder or inhomogeneity. This spectral broadening is more obvious in the ^{23}Na spectra immediately below $T_{\rm AF}$ (Fig. 2a), indicating incommensurate modulation of the hyperfine field. However, the spectral shape changes gradually to rather normal discrete peaks at lower temperature, pointing to an incommensurate-commensurate crossover. Since the broadening is observed only for $H \parallel c$, the hyperfine fields at the As/Na sites should still be almost parallel to the c axis, $\boldsymbol{H}_{\rm hf} = (0, 0, \pm\Delta)$. The spectral shape then represents the spatial distribution of Δ or the AF moments. Therefore, the NMR spectra near $T_{\rm AF}$ indicate a longitudinal SDW order at some incommensurate wave vector.

To illustrate the real-space image of moment distribution, we assume a periodic modulation of Δ between zero and $\Delta_{\rm max}$ along x over the wave length λ. The spectral intensity for $H \parallel c$ as a function of Δ is given as

$$I(\pm\Delta) \propto \left| \frac{d\Delta(x)}{dx} \right|^{-1}. \qquad (3)$$

Integrating the experimental spectra, therefore, gives the relation between Δ and x,

$$x = \frac{\lambda}{2} \frac{\int_0^{\Delta} I(\Delta')d\Delta'}{\int_0^{\Delta_{\rm max}} I(\Delta')d\Delta'}. \qquad (4)$$

By converting Δ to the AF moment, the spatial distribution of AF moments reproduced by ^{23}Na-NMR is obtained as shown in Fig. 3 at various temperatures. At low temperatures, the AF moment is nearly uniform over most of the space and the rapid change occurs only in a narrow region. Such a profile can be regarded as usual C-AF domains separated by domain walls. Near $T_{\rm AF}$, however, the domain wall gets significantly broadened,

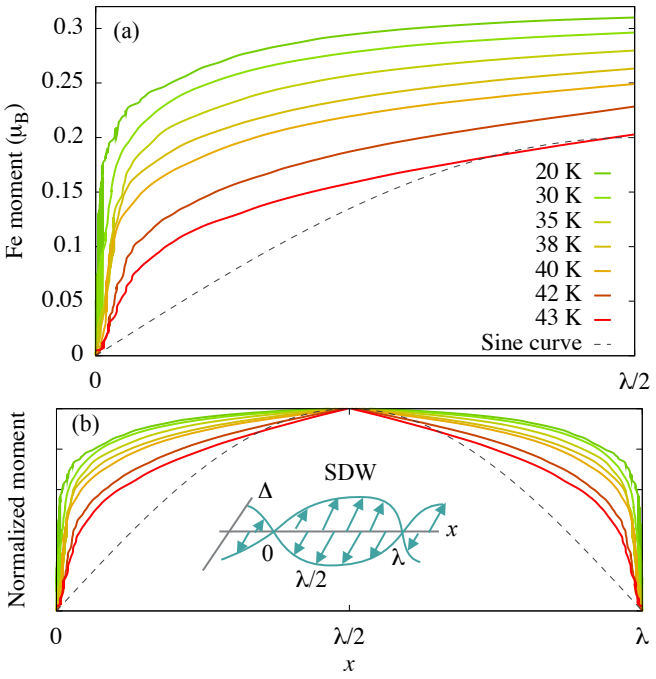

Fig. 3. (Color online) Spatial distribution of Fe moments in the AF state of NaFeAs, assuming the simple periodicity (see text). The panel (a) corresponds to the region $0 < \Theta < \pi/2$ in the schematic in (b). (b) The temperature dependence of the SDW patterns, illustrated by normalizing the data in (a).

making the profile closer to a sinusoidal SDW. The microscopic mechanism for such IC-C crossover is still an open question.

The IC-SDW order at $(1+\delta, 0, \frac{1}{2})_{\rm O}$ or $(1, \delta, \frac{1}{2})_{\rm O}$ breaks cancellation of the a-component of the hyperfine field,[13] therefore, should broaden the NMR spectra for $H \perp c$. The full-width of the spectrum for $H \perp c$ due to incommesuration is given by $\sim 8B_{\rm aa}\sigma\tan(\pi\delta)$, where $B_{aa} (\simeq {}^{75}A^{ab}/4)$ is the diagonal element of the hyperfine coupling tensor determined from the Knight shifts described below. The observed width (0.02 T at 43 K) then puts an upper limit for δ, $|\delta| < 0.004$. Such tiny deviation from commensuration might be difficult to detect by diffraction experiments. Similar observation was reported for Co-doped $BaFe_2As_2$.[6] We cannot rule out, however, interlayer modulation $(1, 0, \frac{1}{2}+\delta)_{\rm O}$ with larger δ.

We note that an IC-C crossover has been observed in $SrFe_2As_2$ under high pressure near 5.4 GPa, where AF and SC states coexist, most likely forming nano-scale hybrid structure.[15] The ^{75}As NMR spectra from AF region show commensurate peaks at low-T but broad distribution at high-T with a crossover near 18 K. Thus the incommensurate stripe order may not be exceptional but common in iron-based materials, in particular, in the vicinity of superconducting phases when $T_{\rm AF}$ is depressed below 50 K.

We next discuss the results in the paramagnetic state. The Knight shifts K ($= H_{\rm eff}/H$) at the ^{75}As and ^{23}Na nuclei are plotted against temperature in Fig. 4 after correcting for the second order quadrupole effects. The Knight shifts at the Na sites are small, of the order of the

dipolar field from Fe moments. By plotting K at the As sites against the susceptibility (the inset of fig. 4), we obtain the diagonal elements of the hyperfine coupling tensor: $^{75}A^c = 2.61 \pm 0.02$ T/μ_B, $^{75}A^{ab} = 3.87 \pm 0.07$ T/μ_B.

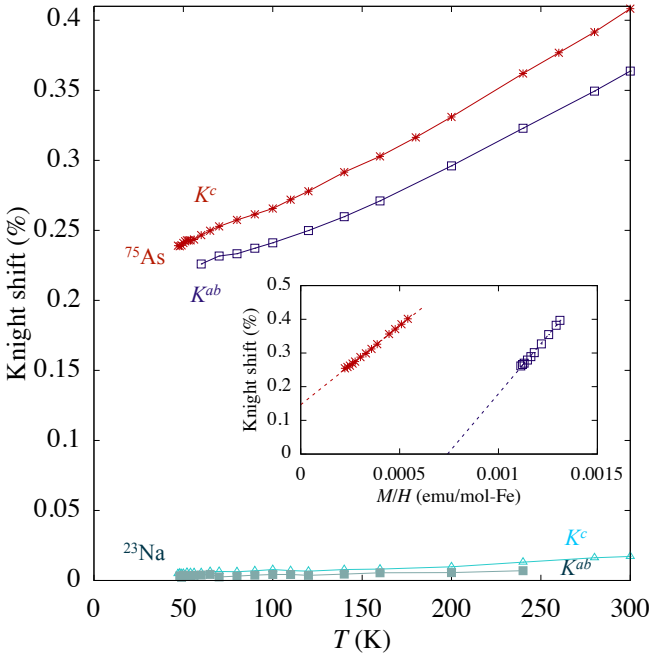

Fig. 4. (Color online) Knight shifts in the paramagnetic state. The inset shows the K versus χ plots for the As sites (low-T data below 70 K have been omitted since M/H showed upturns caused by impurities).

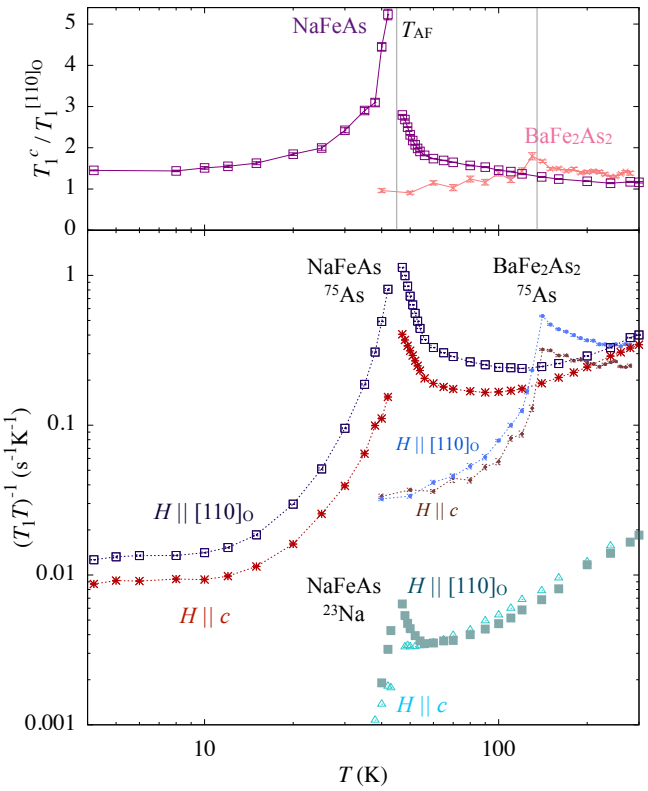

Fig. 5. (Color online) The lower panel shows the spin-lattice relaxation rate divided by temperature $(T_1T)^{-1}$ in NaFeAs, and BaFeAs[13] for two directions of the field. Upper panel shows the anisotropy $T_1^c/T_1^{[110]}$ of the ^{75}As-NMR.

The lower panel of Fig. 5 shows the temperature dependence of the relaxation rate divided by T. The Korringa law, $(T_1T)^{-1} \sim const.$, is observed at the lowest temperatures both in NaFeAs and in 122 compounds,[13,14] indicating that a part of the Fermi surface survives in the AF state even in the presence of a SDW gap. The divergence of $(T_1T)^{-1}$ in NaFeAs near T_{AF} is compatible with a second order transition. Then the nuclear relaxation should be dominated by the stripe AF fluctuations near the wave vector $\boldsymbol{Q} = (1, 0, \frac{1}{2})_O$. The anisotropic ratio of the relaxation rate $(T_1^{[110]})^{-1}/(T_1^c)^{-1}$ provides a measure of anisotropy of the AF fluctuations in spin space,[14]

$$\frac{(T_1^{[110]})^{-1}}{(T_1^c)^{-1}} = \frac{2|S^a(\boldsymbol{Q}, \omega_{\rm res})|^2 + |S^c(\boldsymbol{Q}, \omega_{\rm res})|^2}{2|S^c(\boldsymbol{Q}, \omega_{\rm res})|^2}, \qquad (5)$$

where $|S^i(\boldsymbol{Q}, \omega_{\rm res})|^2$ is the power spectrum of the spin fluctuation along the i-direction at $\boldsymbol{Q}$ and the NMR frequency $\omega_{\rm res}$. The upper panel of Fig. 5 shows divergent behavior of the ratio $(T_1^{[110]})^{-1}/(T_1^c)^{-1}$ of ^{75}As-NMR, which translate into the development of strong anisotropy of the AF fluctuations $|S^a(\boldsymbol{Q}, \omega_{\rm res})| \gg |S^c(\boldsymbol{Q}, \omega_{\rm res})|$. In $BaFe_2As_2$ the divergence is interrupted by the first order transition.

In summary, we have investigated the structural and magnetic transitions and AF spin structure in NaFeAs using ^{75}As- and ^{23}Na-NMR. The NMR relaxation data prove the second-order nature of the AF transition and the strong anisotropy of the AF fluctuations in spin space. The most remarkable feature of the AF state is the temperature-driven crossover from the high-T incommensurate structure to the low-T commensurate structure. This must be an intrinsic feature of a clean and stoichiometric system, as demonstrated by the very sharp NMR spectra and phase transitions of our crystal.

We thank N. Katayama, Y. Kiuchi, and the Materials Design and Characterization Laboratory in ISSP for experimental supports. This work was supported partly by the Grant-in-Aid for Scientific Research (B) (No. 21340093) from JSPS and by the GCOE program from MEXT Japan.

1) K. Ishida, Y. Nakai, and H. Hosono: J. Phys. Soc. Jpn. **78** (2009) 062001.
2) I. I. Mazin, D. J. Singh, M. D. Johannes, and M. H. Du: Phys. Rev. Lett. **101** (2008) 057003.
3) M. D. Lumsden and A. D. Christianson: J. Phys.: Condens. Matter **22** (2010) 203203.
4) J. Wen, G. Xu, Z. Xu, Z. W. Lin, Q. Li, W. Ratcliff, G. Gu, and J. M. Tranquada: Phys. Rev. B **80** (2009) 104506.
5) W. Bao, Y. Qiu, Q. Huang, M. A. Green, P. Zajdel, M. R. Fitzsimmons, M. Zhernenkov, S. Chang, M. Fang, B. Qian, E. K. Vehstedt, J. Yang, H. M. Pham, L. Spinu, and Z. Q. Mao: Phys. Rev. Lett. **102** (2009) 247001.
6) Y. Laplace, J. Bobroff, F. Rullier-Albenque, D. Colson, and A. Forget: Phys. Rev. B **80** (2009) 140501.
7) P. Bonville, F. Rullier-Albenque, D. Colson, and A. Forget: Euro. Phys. Lett. **89** (2010) 67008.

8) G. Chen, W. Hu, J. Luo, and N. Wang: Phys. Rev. Lett. **102** (2009) 247004.
9) S. Borisenko, V. B. Zabolotnyy, D. V. Evtushinsky, T. K. Kim, I. V. Morozov, A. N. Yaresko, A. A. Kordyuk, G. Behr, A. Vasiliev, R. Follath, and B. Büchner: cond-mat/1001.1147v1 .
10) J. H. Tapp, Z. Tang, B. Lv, K. Sasmal, B. Lorenz, P. C. W. Chu, and A. M. Guloy: Phys. Rev. B **78** (2008) 060505(R).
11) W. Yu, L. Ma, J. Zhang, G. F. Chen, T.-L. Xia, S. Zhang, and Y. Hou: cond-mat/1004.3581v1 .
12) S. Li, C. de la Cruz, Q. Huang, G. F. Chen, T.-L. Xia, J. L. Luo, N. L. Wang, and P. Dai: Phys. Rev. B **80** (2009) 020504(R).
13) K. Kitagawa, N. Katayama, K. Ohgushi, M. Yoshida, and M. Takigawa: J. Phys. Soc. Jpn. **77** (2008) 114709.
14) K. Kitagawa, N. Katayama, K. Ohgushi, and M. Takigawa: J. Phys. Soc. Jpn. **78** (2009) 063706.
15) K. Kitagawa, N. Katayama, H. Gotou, T. Yagi, K. Ohgushi, T. Matsumoto, Y. Uwatoko, and M. Takigawa: Phys. Rev. Lett. **103** (2009) 257002.

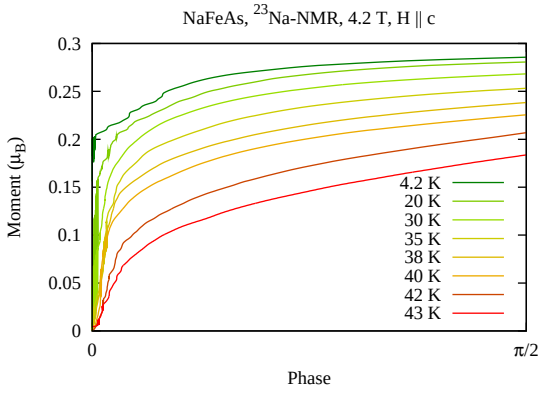
NaFeAs, 23Na-NMR, 4.2 T, H || c
Moment (μB)
0.3
0.25
0.2
0.15
0.1
0.05
0
0
π/2
Phase
4.2 K
20 K
30 K
35 K
38 K
40 K
42 K
43 K